




Investigating the potential for a commercial fishery in the Northeast Atlantic utilizing mesopelagic species

Eduardo Grimaldo ^{1*}, Leif Grimsmo¹, Paula Alvarez², Bent Herrmann¹, Guro Møen Tveit¹, Rachel Tiller¹, Rasa Slizyte¹, Naroa Aldanondo², Trude Guldborg³, Bendik Toldnes¹, Ana Carvajal¹, Marte Schei¹, and Merethe Selnes¹

¹SINTEF Ocean, Brattørkaia 17C, N-7010 Trondheim, Norway

²AZTI Technalia, Herrera Kaia, Portualdea z/g, 20110 Pasaia, Gipuzkoa

³SINTEF Industry, P.O. Box 4760 Torgarden, NO-7465 Trondheim, Norway

*Corresponding author: tel: + 47 40 624 014; e-mail: eduardo.grimaldo@sintef.no.

Grimaldo, E., Grimsmo, L., Alvarez, P., Herrmann, B., Møen Tveit, G., Tiller, R., Slizyte, R., Aldanondo, N., Guldborg, T., Toldnes, B., Carvajal, A., Schei, M., and Selnes, M. Investigating the potential for a commercial fishery in the Northeast Atlantic utilizing mesopelagic species. – ICES Journal of Marine Science, doi:10.1093/icesjms/fsaa114.

Received 9 April 2020; revised 9 June 2020; accepted 10 June 2020.

During three cruises in the Mid Atlantic Ridge area in 2016 and 2017, we studied the biomass of mesopelagic fish and its potential as a source of protein and oil for animal feed and human consumption. We collected samples of mesopelagic species down to a depth of 600 m, studied fish behaviour, identified and quantified the species composition of the catches, analysed the chemical composition of the catch samples, and evaluated the presence of unwanted substances. Results showed that *Maurolicus muelleri* (Mueller's pearlside) and *Benthosema glaciale* (Glacier lantern fish) were the most abundant fish species in our samples and catches containing 80% fish can be a good source of protein and marine lipids including eicosapentaenoic acid (C20:5n3) and docosahexaenoic acid (C22:6n3). Unwanted substances, except for Cd and As, were present at levels far lower than the limits set by European Union regulations. However, our experiments identified challenges that may limit the efficiency of commercial operations in the Northeast Atlantic. Combined real-time optical and/or multifrequency acoustic systems will be needed to improve species identification and ensure cost-effective fishing operations. Also, selective trawls that target only fish and release unwanted species are needed to secure high-quality oils and proteins.

Keywords: chemical composition, commercial fishery, feed, marine lipids, *Maurolicus muelleri*, mesopelagic fish, protein, scattering layer, siphonophore

Introduction

The mesopelagic layer of the ocean at depths between 200 and 1000 m is inhabited by a large variety of species (Dalpadado *et al.*, 1998), and mesopelagic species have been viewed as a potential harvestable resource since the 1970s (Gjøsæter and Kawaguchi, 2002; FAO 1997; 2014). Some of these species have been considered suitable for human consumption, but

mostly they are aimed at supplying raw material to the fish meal and oil industry (Olsen *et al.*, 2010). This is an important resource at a time when the demand for feed for the aquaculture industry is increasing and the supply of marine oils containing marine omega-3 fatty acids (FAs) eicosapentaenoic acid (EPA) and docosahexaenoic acid (DHA) is deficient. Marine lipids have been partially replaced in fish feed by

lipids from land-based sources (i.e. soybeans), but the replacement level for the salmon industry has reached its maximum (Naylor *et al.*, 2009; FAO, 2014). If exploited at sustainable levels without impacting the biodiversity and/or compromising the oceans' role in climate regulation, the biomass of mesopelagic species may be a potential source of polyunsaturated FAs (PUFAs) and high nutritional value proteins to meet aquaculture demands and provide human nutrition (FAO, 2016).

Marine long chain omega 3 FAs (DHA and EPA) provides health benefits for humans, animals and fish in general. However, currently the omega-3 derived from wild fish is not enough to meet the needs of a growing population and aquaculture industry. Therefore, new sources of marine omega-3 are needed. Mesopelagic fishes' high abundance estimates present an opportunity to reduce the shortage of omega-3 and the supply of these essential FAs for the market. This is especially true when results show that according to Alvheim *et al.* (2020) mesopelagic species caught in fjords in western Norway have been reported to contain up to 30% of omega-3 FAs (% of total FAs): *Benthosema glaciale* (22.5 ± 3.1), *Maurolicus muelleri* (17.5 ± 3.5), *Meganyctiphanes norvegica* (29.7 ± 5.7), *Pasiphaea sp.* (26.4 ± 3.0), *E. arcticus* (24.3 ± 1.9) and *Periphylla periphylla* (3.3).

Mesopelagic fish and krill are widely distributed in the ocean though and despite being two of the largest known marine resources globally, they are still under-exploited commercially and little is known about them. In fact, global estimates of the mesopelagic fish biomass alone vary widely from 1 to 10 billion tonnes (Gjøsæter and Kawaguchi, 2002; Irigoien *et al.*, 2014; Proud *et al.*, 2019), including the Northeast Atlantic (NEA) and the Economic Exclusive Zone of adjacent nations (Gnaiger and Bitterlich, 1984; Sigurdsson *et al.*, 2002; Anderson *et al.*, 2005). We do know though that the Myctophidae and Sternoptychidae are two of the most abundant families of mesopelagic fish globally (Valinassab *et al.*, 2007). *Maurolicus muelleri* (Mueller's pearlside) is a small (4–5 cm), short-lived mesopelagic fish reported from most of the world's continental slopes areas. Although they can reach the age of 4–5 years, only a small proportion of the population reaches the age of 3 years (Gjøsæter, 1981), and in areas such as the Rockall Trough longevity may only be closer to 1 year (Kawaguchi and Mauchline, 1982, 1987). The spawning season lasts from March to September in Norwegian waters (Lopes, 1979; Gjøsæter, 1981; Goodson *et al.*, 1995), and a wide geographic distribution and long spawning period indicate a greater tolerance to variations in hydrographic conditions (Gamulin and Hure, 1985; Zenteno *et al.*, 2014).

Mesopelagic fish are important prey for higher trophic levels (Naito *et al.*, 2013) and a key component of the biological carbon pump through diel vertical migrations (DVMs) (Dypvik *et al.*, 2012; Klevjer *et al.*, 2016). Its value as such goes beyond its harvestable potential. However, despite the varied projections of a potentially large biomass of mesopelagic fish, they are one of the least investigated components of the marine ecosystem, with major knowledge gaps about their biology and ecology (Hidalgo and Browman, 2019). In gyres, the mesopelagic biomass appears to be related both to production and concentration by currents (Benitez-Nelson *et al.*, 2007; Godø *et al.*, 2012), while in other areas, such as the southern Icelandic shelf and the area over the Reykjanes Ridge, advective processes seem to be the ultimate force gathering thinly distributed resources into biomass hotspots (Sigurdsson *et al.*, 2002; Sutton *et al.*, 2008). DVM is common for many mesopelagic species (Kaartvedt *et al.*, 2008, 2011, 2012;

Staby and Aksnes, 2011; Dypvik *et al.*, 2012; Klevjer *et al.*, 2016) and by migrating from the ocean depths to the epipelagic zone to feed, these animals effectively transport carbon into the deep mesopelagic zone (Davison *et al.*, 2013).

Understanding the spatial-temporal variability of the mesopelagic biomass is critical to assess the degree to which it is possible to exploit it sustainably within the context of its role in the marine food web. Current challenges to studying mesopelagic scattering layers centre on collecting representative samples. While small-meshed plankton nets can be avoided by large fish, midwater trawls can be selective and do not sample the whole community. Hence, midwater trawls are inefficient at sampling siphonophores because these fragile organisms are easily destroyed (Geoffroy *et al.*, 2019). Additionally, how resonance and DVM bias the estimation of the mesopelagic biomass is unknown. Some mesopelagic species have strong acoustic target strength, such as gas-bladdered fish and gas-bearing siphonophores; they are strong acoustic targets and therefore are mostly responsible for the mesopelagic backscatter (Godø *et al.*, 2009; Peña *et al.*, 2014; Kloser *et al.*, 2009, 2016; Scouling *et al.*, 2015). These species are also highly resonant in deep waters at 38 kHz (Kloser *et al.*, 2016; Proud *et al.*, 2019). Although trawl avoidance by mesopelagic fish may lead to great underestimation of their biomass by net sampling (Kaartvedt *et al.*, 2012), the acoustic energy is also not necessarily directly proportional to fish biomass (Proud *et al.*, 2019). Trawling seems to enhance the presence of gas-bladdered fish in the catches, while optical measurements highlight the depth distribution and biomass of gas-bearing siphonophores (Kloser *et al.*, 2016; Proud *et al.*, 2019).

The main objectives of this study were to fill some of the knowledge gaps associated with mapping the spatial-temporal distribution of mesopelagic species in international waters along the Mid Atlantic Ridge to assess these species as a potential source of protein and oil for animal feed and human consumption. The specific objectives of the field trials were to collect samples of mesopelagic species down to 600 m depth, study fish behaviour in relation to the catching process, identify and quantify the species composition of the catches, analyse the chemical composition (including FA and lipid class composition) of catch samples, and analyse the presence of unwanted substances.

Material and methods

Data were collected during three cruises that were carried out in the Mid Atlantic Ridge on 27 June 2016–29 July 2016 (cruise 1), 18 April 2017–11 May 2017 (cruise 2), and 11 July 2017–4 August 2017 (cruise 3) (Figure 1). We used the 62 m long commercial pelagic trawler “MS Birkeland” instrumented with a Sonic Kaijo Denki KSE 300 sizing echosounder with a 38 kHz transducer (www.u-sonic.co.jp); Kayo Denki fisheries search sonars (types KCS–228Z, 24 kHz and KCH–1828, 160 kHz); and Simrad trawl sonar, type FS20/25, 90 kHz horizontal and 120 kHz vertical sonar heads. Acoustic instruments were used to search for mesopelagic concentrations, but we had no equipment for logging acoustic data from these cruises.

Sampling trawls, trawl sensors and optical monitoring equipment

Two midwater trawls, one with a 1200 m and the other with an 800 m circumference, were used to collect samples of

mesopelagic species in 2016 and 2017, respectively. A series of 20 and 16 mm small-meshed nets were attached inside the trawl extension piece to avoid escape of mesopelagic fish. These mesh sizes were chosen as a compromise between maximizing the trawl's catch area and reducing the total drag of the trawl. Under operation, the mouth opening of the trawl was 90-m wide and 50-m high and the cross-sectional area of the trawl blinded with 16 mm meshes was 130 m². The mouth opening of the 800 m trawl was 45 m wide and 40 m high and the cross-sectional area of the trawl that had 20 mm meshes was 1200 m² while that with 16 mm meshes was 130 m². The codend was blinded with small-meshed netting sections of 16- and 12-mm mesh size. The mean \pm standard deviation of the mesh opening of the 12 mm netting was 11.1 \pm 0.2 mm. Based on the acoustic backscattering we collected samples in the layer with the strongest backscattering and control the depth of the trawl's headline with the trawl sonar. Simultaneously, the trawl sonar helped monitoring the geometry of the trawl, which was identified by measuring the horizontal and vertical cross-section of the trawl mouth. The height in different parts of the trawl was monitored by Scanmar trawl eye sensors (97 kHz) attached to the trawl's top panel. The tow speed varied between 2.2 and 2.4 knots, and the mean water flow speed measured in the trawl's extension piece was 1.3 \pm 0.1 ms⁻¹ in 2016 and 1.1 \pm 0.1 ms⁻¹ in 2017. Underwater video recording was conducted at all sampling stations to study fish behaviour relative to the trawl, small-meshed sections, and codend. We used two or four GoPro Hero4 Black edition cameras and red/infrared (620–630 nm) lights that provided adequate illumination; these devices were attached inside and outside the trawl's top panel and in different parts along the trawl body, extension piece, and codend. Species identification and the estimation of the number of siphonophores m⁻³ was made using the HD videos (60 frames s⁻¹) and analysing the videos frame by frame using the tool VLC media player. We avoided double counting of organisms by tracking individuals, accounted for the field of view and for the tow speed inside the trawl.

Catch composition and length measurements

Size frequency distribution and cumulative size frequency distribution analyses were used to compare length distributions of the main fish species caught during the cruises. The analysis was done species by species and cruise by cruise as follows: Let n_{il} be the number belonging to length class l of a specific species caught and length measured in fishing haul i during a specific cruise and let q_i be the fraction of the catch of this species that was length measured. Based on this information, the size frequency distribution $D_n l$ and the cumulative size frequency distribution $CD_n L$ were obtained by:

$$D_n l = \frac{\sum_{i=1}^h \left\{ \frac{n_{il}}{q_i} \right\}}{\sum_{i=1}^h \sum_{l=1}^L \left\{ \frac{n_{il}}{q_i} \right\}} \quad (1)$$

$$CD_n L = \frac{\sum_{i=1}^h \sum_{l=0}^L \left\{ \frac{n_{il}}{q_i} \right\}}{\sum_{i=1}^h \sum_{l=1}^L \left\{ \frac{n_{il}}{q_i} \right\}}$$

The summations of i and l in (1) are over the h hauls conducted during the given cruise and length classes l , respectively. $CD_n L$ quantifies the proportion (in number of fish) of the total catch up to a given length class L .

The analysis according to (1) was conducted using the statistical analysis tool SELNET (Herrmann *et al.*, 2012; Melli *et al.*, 2020), and the double bootstrapping technique implemented in this tool was used to estimate 95% confidence intervals (CIs). The double bootstrapping method considered both the between-haul variability in the structure of the population captured in the codend and the within-haul variability due to limited numbers of the species captured in that specific haul, as well as the effect of subsampling (Herrmann *et al.*, 2017). Specifically, the double bootstrap included of an outer resampling loop that accounted

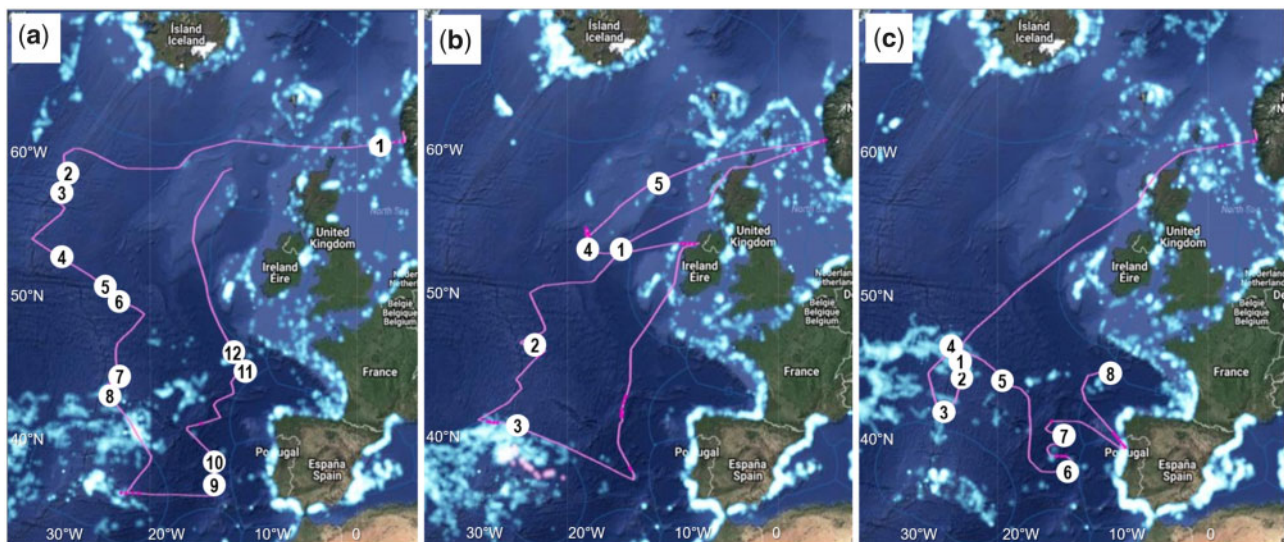


Figure 1. The pink line shows the route followed by the vessel “MS Birkeland” in (a) June 2016–July 2016 (cruise 1), (b) April 2017–May 2017 (cruise 2), and (c) July 2017–August 2017 (cruise 3). The circles indicate the haul number.

for between-haul variability by selecting hauls with replacement from the total number of hauls conducted during the specific cruise. The selected number of hauls in the outer resampling loop equalled the total number of hauls conducted during the specific cruise. Within-haul uncertainty was accounted for in an inner loop by resampling the catch of the species for each of the hauls selected in the outer loop. The number resampled for the individual hauls in this inner loop equalled the total number of individuals of the species length measured in the catch for each of the selected hauls. The resampled catch was subsequently raised according to the sampling ratio q_i for the specific species and specific haul to account for the additional uncertainty caused by subsampling following the procedure described by Eigaard *et al.* (2012). One thousand bootstrap repetitions were conducted and used to estimate the 95% Efron percentile CIs (Efron, 1982) for D_{nI} and CD_{nL} .

Age and growth analysis

One haul from 2016 and three hauls from 2017 were selected for biological studies. In the laboratory, total length (TL) and standard length (SL) of individuals were measured to the nearest 0.1 mm, and total weight and gonad weight were obtained before otolith extraction. Additionally, the gonads were analysed macroscopically to determine both the sex and the sexual maturity status following Walsh *et al.* (1990). Allometric relationships were established between TL and SL and between SL and body weight.

Otoliths were read on an annual and daily scale. For daily growth, when available, five individuals for each 0.5 cm SL range were processed to obtain a representative sample of the whole range of lengths. The otoliths were extracted from the saccular chamber under a binocular dissecting microscope. Both sagittal otoliths were removed from each sample, although only the right otoliths were used for growth analyses. Otoliths were mounted singly on slides with a drop of Crystalbond thermoplastic glue under a dissecting microscope. They were subsequently ground down with a 0.3 μ m lapping film from one side and, after reheating and repositioning the other side, the same process was repeated until the nucleus and all increments were sufficiently visible. Otoliths were analysed using a light microscope coupled with an image analyser (Visilog, TNPC Software, v.5.02, Ifremer, Issy-les-Moulineaux, France). The central part of each otolith was read at $\times 1000$ magnification in immersion oil, and the outer part was analysed at $\times 200$ magnification. Composite image files were constructed to enable the reader to scroll across the complete otolith image during analysis. All increments were counted, and the distance between increments was measured along the longest axis from the core to the edge of the otolith on the post-rostrum side. Increments were assumed to be daily from the first increment (Boehlert *et al.*, 1994; Folkvord *et al.*, 2016). Additionally, hatch date was calculated by subtracting otolith increment counts from the day that individuals were collected in the field. Each otolith was read twice by the same reader. Any otolith with a difference between readings higher than 5% was rejected. All of the 32 otoliths read were used in the analysis.

Biochemical analyses

From each trawl station three 1000 g samples containing representative unsorted raw material, were taken randomly from the codend immediately after the trawl was taken onboard and frozen at -25°C . We used unsorted catch for the biochemical analyses

because we expect that future mesopelagic fishery most likely will be a mix of different species. The moisture content (MC) was determined gravimetrically after drying for 24 h at 105°C until constant weight was achieved. Ash content was determined according to AOAC (1990). Total nitrogen (N) was determined using an ECS 4010 Nitrogen/Protein Analyzer (Costech Analytical Technologies Inc., Valencia, CA, USA), and crude protein was estimated by multiplying total N by a factor of 6.25 (Gnaiger and Bitterlich, 1984; Sosulski and Imafidon, 1990). The Bligh and Dyer (1959) method was used for extraction of lipids. The FA composition of the lipids was determined by gas-liquid chromatography of FA methyl esters as described by Daukšas *et al.* (2005). Two replicates of methylation and gas chromatography analysis were also performed, and the results were expressed in mg FA/g sample and percentage of each FA to total FA. The lipid classes were determined by thin-layer chromatography with a flame ionization detector system (Iatroscan TLC-FID analyser TH-10 MK-IV, Iatron Laboratories Inc., Tokyo, Japan) according to the method of Fraser *et al.* (1985) as described by Šližytė *et al.* (2005). In total, four replicate analyses were performed, and the results were expressed in area % as the mean value.

Analysis of unwanted substances

Five 2000 g samples of unsorted raw material (two samples from 2016 and three from 2017) were analysed for content of unwanted substances such as dioxins, polychlorinated biphenyls (PCBs), polycyclic aromatic hydrocarbons (PAHs), pesticides, and heavy metals [lead (Pb), cadmium (Cd), mercury (Hg), and arsenic (As)]. Dioxins and PCBs were analysed by Eurofins GfA Lab Service GmbH (Hamburg, Germany), and PAHs, pesticides, and heavy metals were analysed by Eurofins WEJ Contaminants GmbH (Hamburg, Germany). The analyses were conducted in accordance with the EU official methods for the determination of heavy metals in feedstuff and foodstuff (EC, 2012a), and the results were compared with the maximum limits of unwanted substances in animal feedstuff (EC, 2002, 2011, 2012b) based on 12% MC and maximum levels in food wet weight and foodstuffs (EC, 2006, 2014).

Results

Scattering layers and sampling catches

In July 2016 (cruise 1), three sound scattering layers (SSLs) were often present during the daytime (Figure 2, Supplementary File S1). One was located between 100 and 250 m. The second was between 300 and 360 m, and the final one was between 420 and 700 m (Figure 2, Supplementary File S1). Underwater video recordings helped identify the species composition of these layers. The upper most SSL mostly consisted of *M. muelleri*, krill, and different types of small jellyfish, as well as siphonophores (Figure 3 and Supplementary Video S1). Most of these organisms generally displayed limited (or no) swimming ability inside the trawl (except for *M. muelleri* 30 mm) and were easily transported towards the codend. However, the trawl samples collected from these depths did not reflect the expected species composition based on observations from the underwater images, as very few jellyfish and almost no traces of siphonophores were collected. Underwater video recordings showed that the SSL <300 m consisted of a large variety of fish species and large numbers of siphonophores, which in some areas reached up to 80–100 individuals m^{-3} (Figure 3 and Supplementary Video S2). Sampling

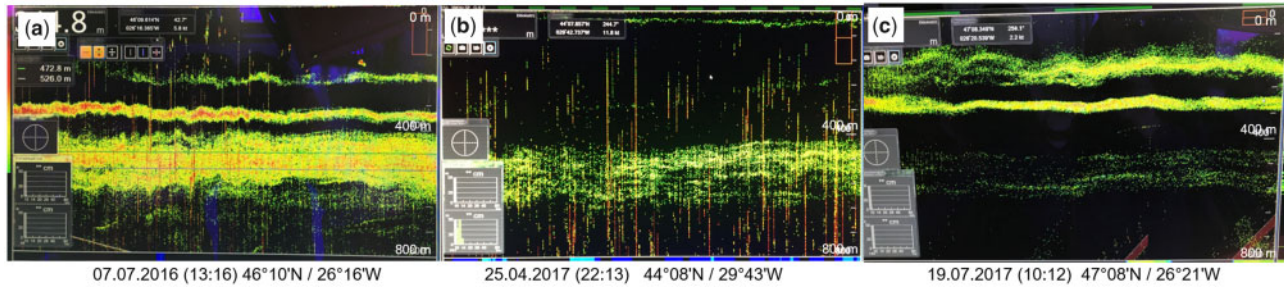


Figure 2. Images of the echosounder screen (38 kHz) with the concentration of mesopelagic organisms in the water column in the Mid Atlantic Ridge during cruise 1 (a), cruise 2 (b), and cruise 3 (c). All images belong to the area 46°–50°N and 21°–26°W.

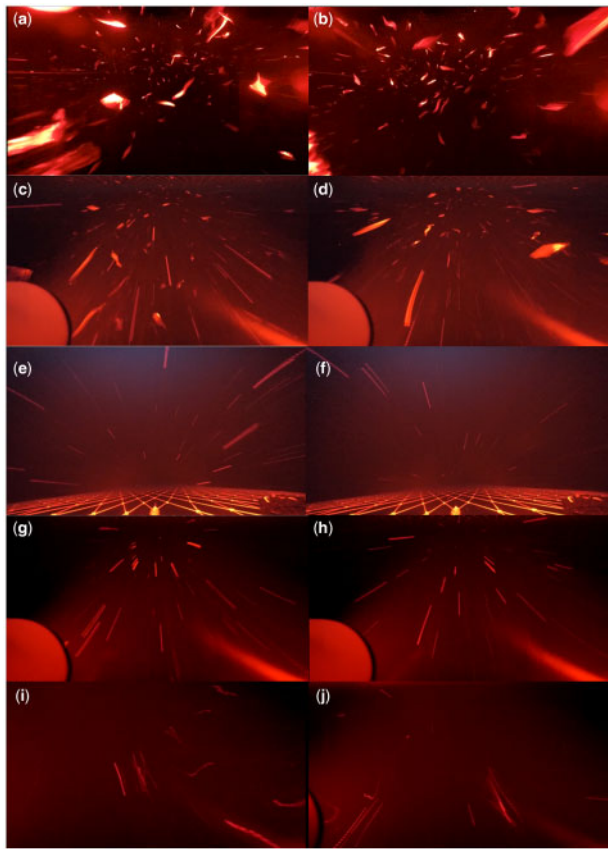


Figure 3. Images (a) and (b) show almost purely *Maurolicus muelleri* inside the trawl's extension piece (sampling station: 1-H06). Images (c) and (d) show a large diversity of mesopelagic organisms inside the trawl's extension piece (sampling station: 1-H05). Images (e) and (f) show large numbers of mesopelagic organisms (not fish) passing through the 200 mm meshes and out of the trawl belly (sampling station: 1-H08). Images (g) and (h) show similar types of organisms inside the trawl's belly (sampling station: 1-H08). Images (i) and (j) show magnified images of siphonophores inside the trawl's extension piece (sampling station 1-H08).

catches from the SSL <300 m yielded a large variety of fish species, krill, and jellyfish but no traces of siphonophores. Of the fish species caught in these depths, *B. glaciale* was the most abundant.

In April–May 2017 (cruise 2), we detected a thin SSL between 70 and 150 m and another between 400 and 600 m (Figure 2, Supplementary File S2). Sampling catches from the SSL at 100 m mostly consisted of *M. muelleri*, while those from the 400 m consisted mostly of krill, *B. glaciale*, and jellyfish. In July 2017–August 2017 (cruise 3), three scattering layers were often present during the daytime. An SSL was located between 100 and 250 m, another between 300 and 400 m, and the last between 420 and 700 m (Figure 2, Supplementary File S3). Underwater video recordings showed that the SSL mostly consisted of *M. muelleri* smaller than 30 mm and that large numbers of fish was sorted out through the 20 mm meshes in the trawl's belly and extension piece. Video recordings also showed that the SSL <300 m consisted of a large variety of fish species and large amounts of siphonophores (up to 20–30 individuals m⁻³). Sampling catches at the SSL yielded a large variety of fish species, krill, and jellyfish but no traces of siphonophores.

In total, 25 sampling hauls were carried out during the three cruises and all of them were carried out during daytime. Five hauls were taken 150 m, 14 hauls occurred at depths between 150 and 400 m, and the remaining 6 hauls were taken deeper than 400 m. The catch rates reached up to 12 tonnes h⁻¹ (station 1–H10) (Table 1). More than 30 mesopelagic species were caught during the three cruises. *M. muelleri*, *B. glaciale*, and krill were the three most abundant species, and representing 98% of the total catch (in weight) (Table 2). Figure 4 shows the length frequency distributions of the two most abundant fish species. Of commercially important fish species, only one 56 cm saithe (*Pollachius virens*) was caught during the three cruises.

Age and growth of *M. muelleri*

A total of 196 individuals of *M. muelleri* that ranged from 15 to 55 mm SL were analysed from four hauls collected in spring and summer 2016 and 2017. Table 3 shows the main characteristics of specimens per haul. The smallest individuals were captured in July 2017 (3–H04), consisting of juvenile (immature) fish. The overall female to male ratio was close to 1:1. In 2016, all fish were mature. In 2017, however, 27% of all fish analysed were immature, and females accounted for 39% and males accounted for 33%.

The relationship between the TL (mm) and SL (mm) was described by:

$$SL = -0.637 (\pm 0.269) + 0.853 (\pm 0.006) TL, \text{ with } R^2 = 0.99; p < 0.001; n = 196.$$

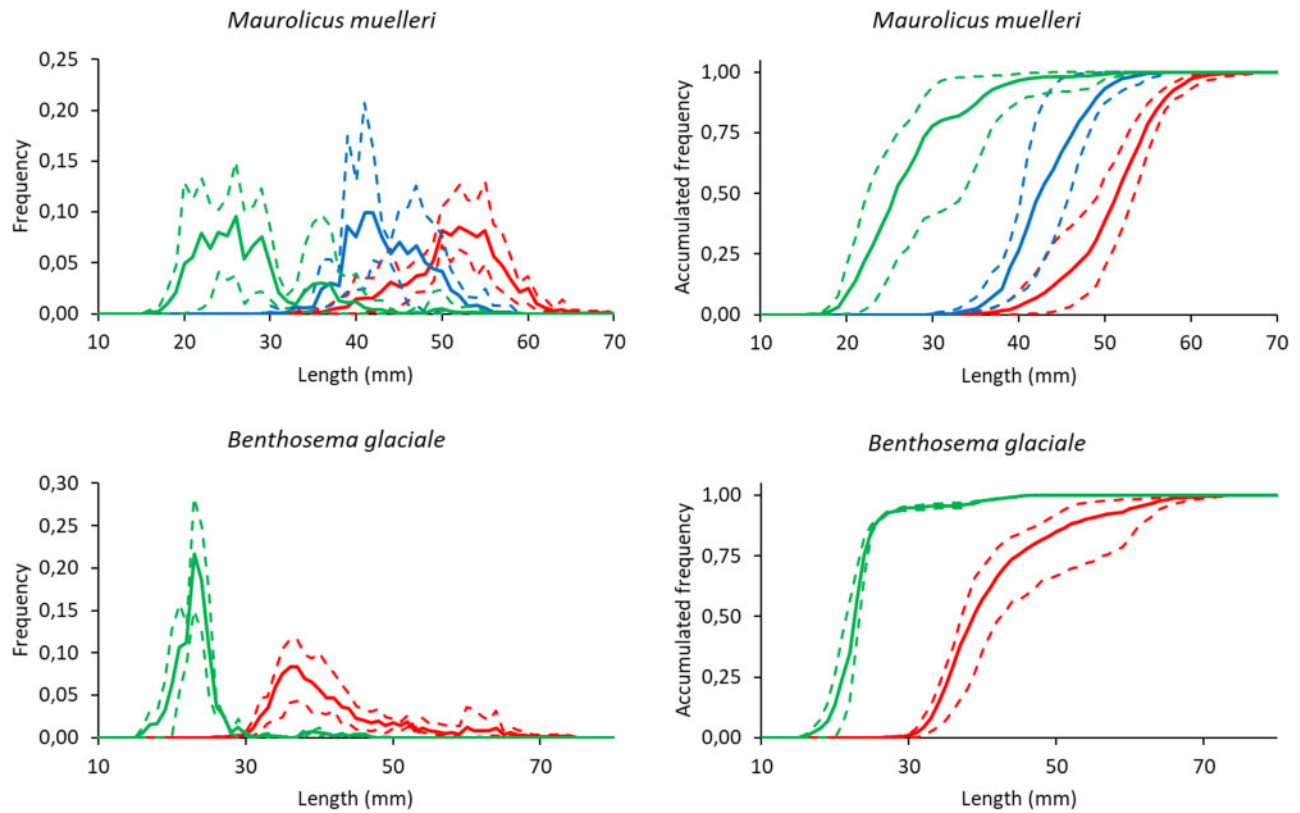


Figure 4. Size frequency distribution (left) and cumulative size frequency distribution (right) of the *Maurolicus muelleri* and *Benthosema glaciale* collected during the cruises (red line for cruise 1, blue line for cruise 2, and green line for cruise 3). Stippled curves represent 95% confidence bands.

Table 1. Operational data and sampling hauls.

Cruise-haul no.	Date	Position	Tow speed (knots)	Tow time (min)	Headline depth (m)	Temp. at fishing depth (°C)	Total catch (kg)	Biomass density ^a g m ⁻³
1-H01	28 June 2016	60°30'N 04°37'W	2.4	30	220	–	4 000	15.94
1-H02	2 July 2016	59°46'N 31°26'W	2.4	60	480	6.2	1 000	1.99
1-H03	3 July 2016	56°30'N 31°27'W	2.2	50	400	–	1 000	2.61
1-H04	4 July 2016	53°46'N 32°00'W	2.2	40	400	5.2	1 000	3.26
1-H05	5 July 2016	52°16'N 25°57'W	2.2	30	400	7.0	1 000	4.35
1-H06	5 July 2016	51°37'N 26°33'W	2.3	15	160	11.8	2 000	16.63
1-H07	7 July 2016	46°33'N 26°01'W	2.3	30	150	13.5	1 000	4.16
1-H08	7 July 2016	46°09'N 26°16'W	2.2	30	500	10.9	500	2.17
1-H09	13 July 2016	37°34'N 19°15'W	2.2	20	470	14.5	100	0.65
1-H10	14 July 2016	38°46'N 15°26'W	2.2	15	250	15.8	3 000	26.08
1-H11	17 July 2016	48°15'N 13°43'W	2.2	15	367	12.8	3 000	26.08
1-H12	18 July 2016	50°28'N 15°37'W	2.3	15	260	16.3	500	4.16
2-H01	21 April 2017	53°51'N 17°19'W	2.2	20	100	11.9	200	1.30
2-H02	24 April 2017	48°13'N 26°19'W	2.2	20	80	12.7	0	0
2-H03	30 April 2017	43°27'N 26°41'W	2.2	60	320	12.5	350	0.76
2-H04	5 May 2017	55°34'N 20°09'W	2.3	45	50	11.4	600	1.66
2-H05	9 May 2017	59°58'N 13°32'W	2.2	45	200	9.1	500	1.45
3-H01	16 May 2017	47°10'N 26°17'W	2.2	120	260	12.6	300	0.33
3-H02	16 May 2017	46°15'N 26°33'W	2.3	45	212	13.2	275	0.76
3-H03	17 May 2017	44°20'N 29°01'W	2.2	50	338	12.6	100	0.26
3-H04	18 May 2017	48°00'N 26°43'W	2.2	50	212	12.3	250	0.65
3-H05	19 May 2017	45°47'N 21°36'W	2.2	60	85	14.3	300	0.65
3-H06	21 May 2017	39°24'N 16°54'W	2.2	50	212	14.8	100	0.26
3-H07	23 May 2017	42°24'N 16°02'W	2.2	60	170	14.1	300	0.65
3-H08	29 May 2017	46°52'N 10°14'W	2.2	30	100	13.6	100	0.43

^aThe biomass density was estimated considering the volume of water filtered by the cross-sectional area of the trawl blinded with 16 mm meshes (130 m^2), the distanced covered by the trawl (m) at a towing speed (transformed to m s^{-1}) the effective tow time (min) and the catch (kg).

The relationship between the total weight (W , g) in the SL is shown in Figure 5a. *M. muelleri* weight ranged from 0.02 to 2.19 g. No statistical difference associated with sex ($p > 0.1$) was detected (Figure 5), so is the adjusted weight–length relationship is described by:

$$W = 0.000013(SL)^{2.97 (\pm 0.036)}, \text{ with } R^2 = 0.97; p < 0.001; n = 196.$$

All *M. muelleri* caught in 2016 belonged to the 1-year class, and 72% of those caught in 2017 belonged to the 0-year class (Figure 5). The average SL for 0-year class individuals was 25.3 ± 4.82 mm and for 1-year class the value was 40 ± 6.13 mm.

SL at age (somatic growth) of *M. muelleri* (Figure 6) is described by:

$$SL = 4.88 + 0.26 d, \text{ with } R^2 = 0.81; p < 0.001; n = 32.$$

The general otolith daily growth pattern revealed that increment widths increased rapidly and were broadest between 38 and 41 d (Figures 6 and 7), with an average maximum value of 8.32 ± 1.30 μm . Thereafter, increment widths decreased.

The 0-year class individuals analysed in this study ranged in age between 46 and 127 d (mean, 79 ± 19 d), corresponding to back-calculated hatch date between 16 March and 4 June. The hatch date frequency distributions indicated that 0-year class *M. muelleri* sampled in July 2017 originated mainly in May (Figure 8) and secondly in the second fortnight of April.

Regarding the reproductive condition, 97% of the analysed *M. muelleri* individuals at < 30 mm TL were immature. By sex and length (Table 4), pre-spawning condition was the dominant stage for individuals 36 mm TL, and the first mature male was observed at 31 mm TL. No females smaller than 30 mm TL were found in the samples, and 29% of the biggest females were spawning.

Gross proximate composition

Table 5 lists the proximate composition of the raw material per cruise-haul. Large variability in the total lipid content was observed, with the highest values in cruise 1. The mean total lipid content varied between 1.4 and 15.8 g 100 g^{-1} , mean protein content ranged from 10.3 to 16.9 g 100 g^{-1} , mean ash content varied from 2.4 to 3.9 g 100 g^{-1} , and mean MC ranged between 68.2 and 83.1 g 100 g^{-1} .

Lipid classes

Samples from 2016 that contained 80% *M. muelleri* (hauls 1–H1, 1–H6, 1–H7, and 1–H10) had a high content (> 75 g 100 g^{-1}) of triglycerides, whereas wax esters (> 67.8 g 100 g^{-1}) were abundant in hauls in which *B. glaciale* was the dominant species (hauls 1–H2, 1–H3, and 1–H4). Oil extracted from samples collected in 2017 contained significant amounts of free FAs, indicating high activity of endogenous enzymes leading to degradation of oils (Table 6).

FA profiles

The FA composition of total lipids from the samples collected in 2016 and 2017 are shown in Tables 7 and 8, respectively. The FAs ranged from C14:0 to C22:6n3. In general, high contents of EPA (C20:5n3) and DHA (C22:6n3) were obtained in all samples from the three cruises. EPA and DHA were the major

Table 2. Catch composition (% in weight) per cruise and haul (cruise number and haul number).

Species	1–H01	1–H02	1–H03	1–H04	1–H05	1–H06	1–H07	1–H08	1–H09	1–H10	1–H11	1–H12	2–H01	2–H03	2–H04	2–H05	3–H01	3–H02	3–H03	3–H04	3–H05	3–H06	3–H07	3–H08
<i>Maurolicus muelleri</i>	86.0	–	–	0.6	26.0	98.0	97.6	19.0	–	99.0	–	–	100.0	–	94.3	22.4	2.6	96.0	2.4	94.2	63.5	99.4	68.2	89.3
<i>Benthosema glaciale</i>	–	95.0	91.0	79.4	50.0	–	–	40.0	55.0	–	–	–	–	12.4	–	–	35.9	–	26.1	–	–	–	–	–
<i>Myctophum punctatum</i>	–	1.0	0.4	1.0	4.0	–	–	2.0	–	–	–	–	–	–	–	–	0.8	–	0.2	–	–	–	–	–
<i>Notoscopelus kroeyeri</i>	–	2.0	1.6	2.0	3.0	–	–	10.0	–	–	–	–	–	–	–	–	–	–	–	–	–	–	–	–
<i>Stomias boa</i>	–	–	1.0	–	2.0	–	–	6.0	–	–	–	–	–	–	–	–	–	–	–	–	–	–	–	–
<i>Arctozenus risso</i>	–	–	–	–	–	–	–	5.0	–	–	–	–	–	–	–	–	–	–	–	1.0	–	–	–	–
<i>Argyropalecus hemigymnus</i>	–	–	–	–	–	–	–	7.0	–	–	–	–	–	–	–	–	0.5	–	–	–	–	–	–	–
<i>Argentina sphyraena</i>	–	–	–	–	–	2.0	2.4	2.0	–	–	–	–	–	–	–	–	–	–	–	–	–	–	–	–
Krill ^a	14.0	2.0	6.0	17.0	15.0	–	–	5.0	45.0	–	100.0	95.0	–	54.7	2.0	77.6	59.0	1.6	71.3	2.4	32.6	–	24.2	10.7
Jellyfish ^a	–	–	–	–	–	–	–	–	–	1.0	–	2.0	–	32.9	1.7	–	–	–	–	–	–	–	–	–
Cephalopods ^a	–	–	–	–	–	–	–	4.0	–	–	–	–	–	–	–	–	–	–	–	–	–	–	–	–
Amphipods ^a	–	–	–	–	–	–	–	–	–	–	–	3.0	–	–	2.0	–	1.2	2.4	–	2.4	3.9	0.6	7.6	–

^aContains more than one species.

PUFAs, while myristic acid (C14:0), palmitic acid (C16:0), and stearic acid (C18:0) were the main saturated FAs. Palmitoleic acid (C16:1), oleic acid (C18:1), arachidic acid (C20:0), and behenic acid (C22:0) were the major monounsaturated FAs.

Table 3. Main characteristic of *Maurolicus muelleri* by cruise and haul.

Variable/cruise-haul	1-H06	2-H04	3-H04	3-H06
SL _{min} (mm)	40	32	15	26
SL _{max} (mm)	55	38	29	35
SL _{mean} (mm)	45.4	34.4	22.13	30.12
Weight _{min} (g)	0.61	0.36	0.02	0.22
Weight _{max} (g)	2.19	0.73	0.26	0.75
Weight _{mean} (g)	1.06	0.49	0.13	0.39
No. males	25	24	5	20
No. females	25	26	2	29
No. indeterminate	0	0	39	1

Undesirable substances

Table 9 lists the undesirable substances found in samples from five hauls collected in 2016 and 2017 (1-H2, 1-H7, 2-H3, 2-H4, and 3-H5). Except for Cd and As, all concentrations of undesirable substances were below maximum limits described by the EU legislation in feedstuff based on 12% MC and maximum levels in feed wet weight.

Discussion

Spatial and temporal variability

The distribution of mesopelagic species in the NEA showed large spatial and temporal variability in 2016 and 2017, as did the density and species composition. The concentrations of *M. muelleri* 50 mm, for example, were extensively distributed over the study area 46°–50°N and 21°–26°W in 2016, whereas fewer and smaller fish were found in the same area in 2017. Similar variability was observed for *B. glaciale* and other organisms for the same years. While most approaches to estimating the abundance of mesopelagic organisms assume that biomass is static in space and time, the results from our cruises show that production seems to

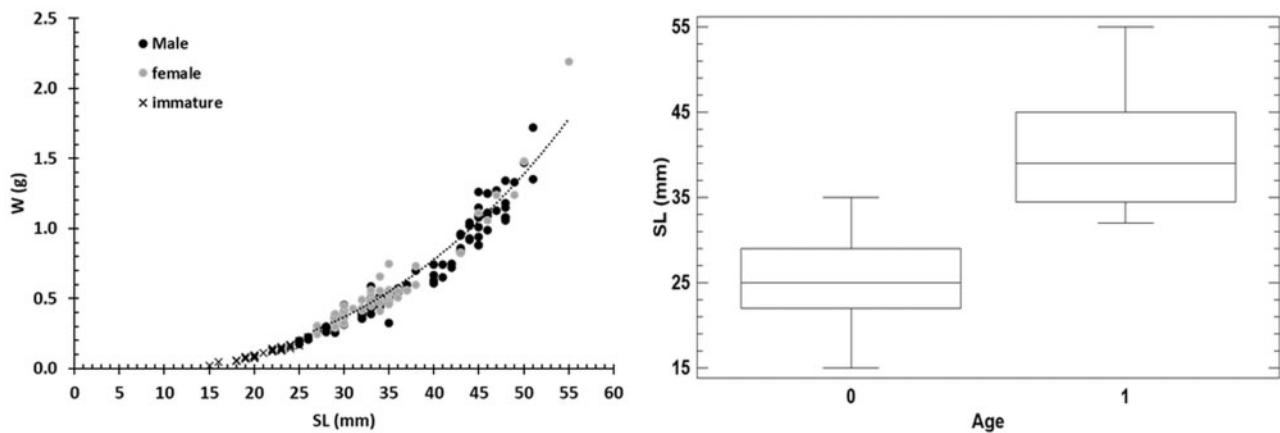


Figure 5. Length-weight relationship (left) and length at age at the annual level (right) for *Maurolicus muelleri*.

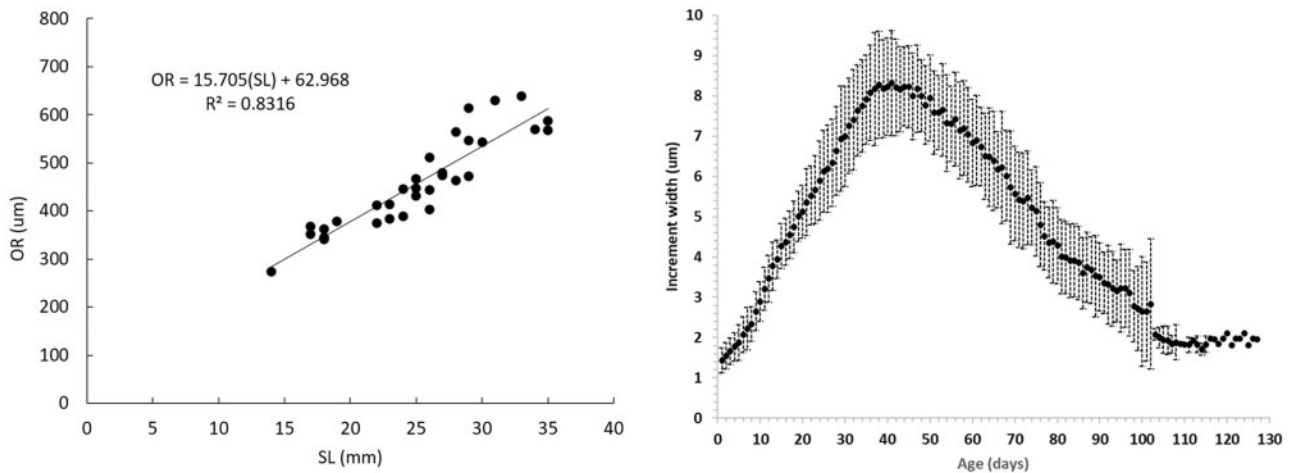


Figure 6. Somatic growth (left) and mean daily growth increments (\pm SD) of 0-year class *Maurolicus muelleri* captured in July 2017 (right).

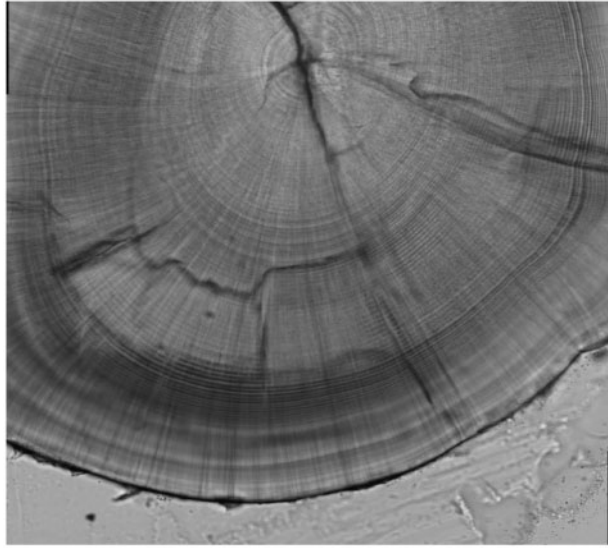


Figure 7. Image of an otolith of *Maurolicus muelleri* showing the daily growth rings from the core to the border. Magnification $\times 20$.

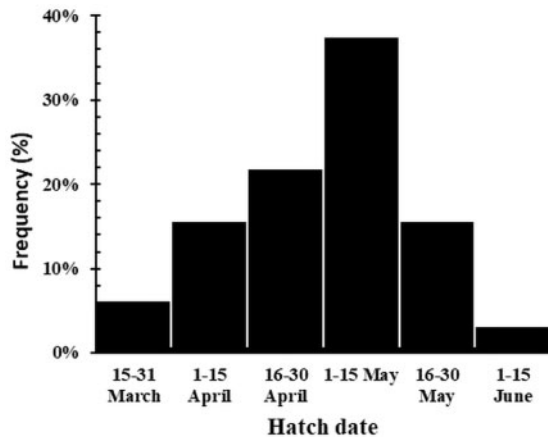


Figure 8. Hatch date frequency distribution of *Maurolicus muelleri* captured in July 2017 (hatch-dates were grouped by fortnight).

fluctuate on different temporal scales in conjunction with changes in spatial distribution. The variability observed in our study is in agreement with that observed in earlier studies documenting seasonal variability, differences in species compositions, and changes in the size structure of the main species of mesopelagic fish at high latitudes (Staby and Aksnes, 2011; Dypvik *et al.*, 2012; Fock and Czudaj, 2019).

Scattering layers, sampling catches, and siphonophores

Despite the interest in exploiting mesopelagic species commercially for food or feed, as well as the known importance of mesopelagic organisms for biogeochemical cycling (Davison *et al.*, 2013; Klevjer *et al.*, 2016), little is known about the large-scale patterns of biomass and proportions of mesopelagic micronekton. Sampling biases differ among net catches, optical observations, and acoustics sampling, and they have been well

Table 4. Maturity stages vs. number of fish in each size class (TL) of male and females.

Stage	Male				Female			
	≤ 30	31–35	36–40	> 41	≤ 30	31–35	36–40	> 41
Immature	1	0	0	0	0	2	0	0
Developed	0	4	0	0	0	0	1	0
Pre-spawning	0	9	24	36	0	9	24	34
Spawned	0	0	0	0	0	0	1	10

Table 5. Gross proximate composition ($\text{g } 100 \text{ g}^{-1}$ fresh weight) in mesopelagic raw material samples (cruise and haul number) collected in 2016 and 2017.

Cruise–haul no.	Lipids	Proteins (Nx6.25)	Ash	Moisture
1–H01	15.81 \pm 0.03	14.96 \pm 0.56	2.43 \pm 0.07	68.20 \pm 0.24
1–H02	11.01 \pm 0.64	14.07 \pm 0.23	2.74 \pm 0.03	72.66 \pm 0.30
1–H03	13.72 \pm 0.36	13.68 \pm 0.45	2.82 \pm 0.07	69.84 \pm 0.21
1–H04	12.04 \pm 0.26	13.99 \pm 1.10	2.94 \pm 0.27	70.46 \pm 0.56
1–H05	12.23 \pm 0.24	14.14 \pm 0.27	2.55 \pm 0.40	70.65 \pm 0.21
1–H06	6.19 \pm 0.17	15.63 \pm 0.48	2.57 \pm 0.08	75.13 \pm 0.11
1–H07	4.34 \pm 0.17	16.91 \pm 0.19	2.87 \pm 0.12	76.01 \pm 0.11
1–H08	7.03 \pm 0.06	13.65 \pm 0.91	3.17 \pm 0.27	75.96 \pm 0.20
1–H09	5.44 \pm 0.01	16.02 \pm 0.66	3.79 \pm 0.13	74.34 \pm 0.31
1–H10	11.11 \pm 0.05	16.67 \pm 1.08	2.83 \pm 0.04	69.82 \pm 0.09
2–H01	1.92 \pm 0.05	15.69 \pm 0.11	2.91 \pm 0.03	80.20 \pm 0.19
2–H03	1.44 \pm 0.03	10.33 \pm 0.10	3.73 \pm 0.11	83.12 \pm 0.33
2–H04	2.63 \pm 0.10	15.36 \pm 0.13	2.83 \pm 0.01	79.33 \pm 0.05
2–H05	3.04 \pm 0.06	16.53 \pm 0.57	3.32 \pm 0.03	76.46 \pm 0.11
3–H01	4.32 \pm 0.08	16.07 \pm 0.28	3.47 \pm 0.07	75.58 \pm 0.24
3–H02	3.23 \pm 0.01	16.44 \pm 0.37	3.39 \pm 0.01	77.56 \pm 0.18
3–H03	3.19 \pm 0.01	13.72 \pm 0.01	3.51 \pm 0.03	79.02 \pm 0.10
3–H04	5.84 \pm 0.03	15.11 \pm 0.17	3.17 \pm 0.10	75.75 \pm 0.11
3–H05	3.67 \pm 0.15	16.42 \pm 0.91	3.44 \pm 0.01	77.13 \pm 0.20
3–H06	9.49 \pm 0.08	16.58 \pm 0.37	2.79 \pm 0.03	71.85 \pm 0.24
3–H07	2.47 \pm 0.01	12.59 \pm 0.23	3.88 \pm 0.01	80.63 \pm 0.05
3–H08	7.84 \pm 0.19	15.62 \pm 0.06	3.00 \pm 0.00	73.73 \pm 0.18

Values are mean \pm standard deviation of two to four samples.

reported for macrozooplankton and micronekton (Kaartvedt *et al.*, 2012; Kloser *et al.*, 2016; Hosia *et al.*, 2017) and were observed in the cruises conducted in this study. Hence, we cannot be certain that trawling will retain all mesopelagic organisms in the water column or if the proportions are representative of the scattering layers. Olsen *et al.* (2019) reported similar results for samples collected in the NEA. Although significant volumes of krill, amphipods, and euphausiids were occasionally caught, these crustaceans are relatively weak scatterers at a frequency of 38 kHz compared with organisms with air-inclusions, and therefore they probably made up a negligible proportion of the total backscatter. As was also reported by Kloser *et al.* (2016), the samples we collected from the scattering layers did not reflect the species composition observed in underwater video footage. This was more evident for the SSL < 300 m, as those catches yielded no traces of siphonophores. We observed very large densities of siphonophores in the NEA 46° – 50° N and 21° – 26° W. At times, the densities of siphonophores along this area reached 80–100 individuals m^{-3} .

Table 6. Lipid classes (g 100 g⁻¹ oil) in samples (cruise and haul number) collected in 2016 and 2017.

Cruise–haul no.	Wax esters	Triglycerides	FFA	Cholesterol	Peak between. Chol. and PL	Phospholipids
1–H01	0.04 ± 0.09	89.88 ± 0.42	0.48 ± 0.07	0.52 ± 0.06	0.16 ± 0.14	8.94 ± 0.57
1–H02	82.31 ± 1.11	4.57 ± 0.67	0.75 ± 0.20	1.01 ± 0.14	0.12 ± 0.08	11.25 ± 0.32
1–H03	85.40 ± 0.37	3.33 ± 0.15	0.67 ± 0.11	0.59 ± 0.06	0.10 ± 0.12	9.91 ± 0.50
1–H04	67.80 ± 2.15	18.18 ± 2.01	1.28 ± 0.28	0.60 ± 0.32	0.45 ± 0.48	11.70 ± 0.33
1–H05	49.20 ± 0.73	36.65 ± 1.30	0.95 ± 0.24	0.91 ± 0.29	0.04 ± 0.09	12.25 ± 1.11
1–H06	0.36 ± 0.11	70.50 ± 1.60	2.19 ± 0.13	2.40 ± 0.36	0.12 ± 0.16	24.44 ± 1.22
1–H07	0.84 ± 0.15	52.21 ± 1.15	4.37 ± 0.21	4.27 ± 0.68	0.05 ± 0.10	38.27 ± 0.56
1–H08	56.98 ± 0.62	24.84 ± 0.45	1.84 ± 0.27	1.40 ± 0.39	0.10 ± 0.11	14.85 ± 0.69
1–H09	52.00 ± 0.40	73.72 ± 0.60	3.88 ± 0.11	3.09 ± 0.56	0.41 ± 0.32	18.90 ± 0.77
1–H10	0.00 ± 0.00	81.94 ± 1.13	1.54 ± 0.39	1.44 ± 0.16	0.25 ± 0.05	14.84 ± 1.39
2–H01	1.48 ± 0.23	8.18 ± 0.29	33.03 ± 1.02	16.21 ± 0.40	–	41.11 ± 0.42
2–H03	29.36 ± 0.71	5.04 ± 0.83	21.07 ± 0.49	10.61 ± 0.44	0.30 ± 0.05	33.63 ± 1.36
2–H04	1.72 ± 0.36	27.85 ± 0.45	35.89 ± 3.98	11.35 ± 1.22	–	23.20 ± 2.56
2–H05	0.62 ± 0.09	54.39 ± 1.66	21.59 ± 1.93	6.25 ± 1.18	0.43 ± 0.43	17.07 ± 1.38
3–H01	35.75 ± 1.31	20.64 ± 1.01	17.88 ± 1.00	5.96 ± 0.94	0.53 ± 0.30	18.69 ± 0.73
3–H02	2.28 ± 0.33	36.97 ± 2.52	25.33 ± 2.55	11.37 ± 1.02	0.28 ± 0.55	23.77 ± 3.76
3–H03	40.15 ± 0.66	11.34 ± 0.97	12.21 ± 1.69	8.35 ± 0.59	–	27.68 ± 2.17
3–H04	0.08 ± 0.16	57.07 ± 2.45	10.36 ± 0.50	5.75 ± 0.34	1.92 ± 0.73	24.83 ± 2.37
3–H05	0.61 ± 0.15	44.80 ± 3.25	15.69 ± 2.35	8.19 ± 1.52	1.18 ± 0.59	29.53 ± 3.49
3–H06	0.00 ± 0.00	77.52 ± 2.94	5.62 ± 0.68	2.64 ± 0.53	0.66 ± 0.62	15.56 ± 2.25
3–H07	1.14 ± 0.16	41.57 ± 4.59	16.52 ± 0.73	8.23 ± 1.09	0.77 ± 0.82	28.01 ± 4.55
3–H08	0.06 ± 0.08	64.26 ± 4.57	3.12 ± 0.71	3.75 ± 1.11	1.26 ± 0.48	27.55 ± 3.55

Values are presented as mean ± standard deviation of four samples.

FFA, free fatty acids; Chol, cholesterol.

Since the density estimates of siphonophores are maximum values and not an averaged water column value, they are not necessarily representative of the area sampled. This concentration of siphonophores is similar though to the maximum values reported by Mills (1995) in the Gulf of Maine, but significantly larger than that reported by Li *et al.* (2012) (>50 individuals m⁻³) in Southeast China, Knutsen *et al.* (2018) (18–20 individual m⁻³) in Northern Norway, and Haberlin *et al.* (2016) (9.8 individuals m⁻³). As pointed out by Kaartvedt *et al.* (2012), trawl avoidance also may have contributed to large underestimation of the mesopelagic biomass and species composition of species collected by net sampling. We observed a certain degree of avoidance in the form of fish herding, especially for large *M. muelleri*. We also observed a large size selection process through the 20 and 16 mm meshes in the trawl's extension and the 11 mm meshes in the codend. Unfortunately, we are unable to provide an estimate of the proportion of small fish selected (removed) from the catches. Contrary to Geoffroy *et al.* (2019), we did not have bycatch of commercially important pelagic species (except for one single saithe), but we did observe herring (*Clupea harengus*) swimming in front of the extension piece. Most pelagic fish species are good swimmers though and probably manage to avoid or escape the trawl because of the low tow speed in our experiments (2.2–2.4 knots) and even lower water flow inside the trawl (1.1–1.3 knots). In summary, we do need more data on the spatial-temporal variability, density, and species composition of mesopelagic fauna, especially in hot spot areas, to determine if the NEA can become commercially important. Future commercial operations targeting the mesopelagic community will need to combine real-time optical and multifrequency acoustic systems that can improve species identification and biomass estimation in order to carry out cost-effective and sustainable fishing operations.

Age and growth

Although the maximum age recorded for *M. muelleri* is 5 years (Armstrong and Prosch 1991), longevity seems to be population dependent. In this study, all individuals of *M. muelleri* belonged to year class 0 or 1, and no fish older than 1 year were captured. Kawaguchi and Mauchline (1982) reported similar results in the Rockall Trough, where they found that longevity may be close to 1 year. In contrast, Gjøsaeter (1981) and Goodson *et al.* (1995) noted that in Norwegian waters individuals reach the age of 3 years but their abundance was scarce. The available information about annual age-at-length in short-lived species such as *M. muelleri*, does not provide much detail about the biology of the population either. For instance, we observed that the 0-year class corresponds to individuals ranging from 16 to 42 mm TL, which agrees, in general, with the ranges described in the literature (Gjøsaeter, 1981; Armstrong and Prosch, 1991). This range of size includes juveniles and adults and mature and immature specimens. Armstrong and Prosch (1991) noted that in the southern Benguela system during the spawning period in May, most of the individuals captured were smaller than 40 mm and belonged to age group 0 (about 260 d). Therefore, “age 0” and “juvenile” for this species do not define the same fraction of the population. We found that 98% of individuals <31 mm TL (=26 mm SL) were immature and therefore juveniles, which coincides with previous results that established lengths of 25 and 21 mm as the separation between juveniles and adults, respectively (Rasmussen and Giske, 1994; Staby and Aksnes, 2011). First maturation length is slightly variable. The smallest mature female observed in our study was 32 mm in TL, which was similar to the length reported by Clarke (1982) and Goodson *et al.* (1995) but different from that reported by Dalpadado and Gjøsaeter (1987), Young *et al.* (1987), and Prosch (1991). Additionally, the composition by age is determined by the life cycle of the population. Kawaguchi and

Table 7. Fatty acid composition (% of total fatty acids) in samples (cruise and haul number) collected in 2016 (cruise 1).

Fatty acid	1-H01 ^a	1-H02 ^b	1-H03 ^b	1-H04 ^b	1-H05	1-H06 ^a	1-H07 ^a	1-H08	1-H09	1-H10 ^a
Total SFA	27.12 ± 0.15	16.05 ± 0.06	13.90 ± 0.04	16.90 ± 0.04	19.37 ± 0.01	26.32 ± 0.06	31.62 ± 0.08	20.00 ± 0.06	32.53 ± 0.15	38.36 ± 0.08
Total MUFA	50.76 ± 0.16	61.91 ± 0.21	55.48 ± 0.16	53.04 ± 0.08	51.30 ± 0.03	46.66 ± 0.11	24.85 ± 0.06	50.93 ± 0.18	39.31 ± 0.37	29.07 ± 0.08
C20:5n3 EPA	5.67 ± 0.01	6.25 ± 0.02	10.14 ± 0.05	9.02 ± 0.03	7.52 ± 0.02	5.08 ± 0.01	9.20 ± 0.01	6.87 ± 0.09	5.77 ± 0.01	5.68 ± 0.01
C22:5n3 DPA	0.70 ± 0.01	0.66 ± 0.01	0.75 ± 0.01	0.81 ± 0.02	0.75 ± 0.01	0.86 ± 0.01	0.98 ± 0.01	0.79 ± 0.01	0.85 ± 0.01	0.72 ± 0.01
C22:6n3 DHA	7.95 ± 0.01	9.39 ± 0.16	12.27 ± 0.09	12.10 ± 0.02	12.58 ± 0.04	14.31 ± 0.07	25.66 ± 0.03	15.36 ± 0.11	16.64 ± 0.13	20.43 ± 0.01
Total PUFA	22.12 ± 0.06	22.04 ± 0.18	30.62 ± 0.13	30.06 ± 0.15	29.33 ± 0.06	27.02 ± 0.07	43.54 ± 0.06	29.06 ± 0.31	28.16 ± 0.13	32.57 ± 0.03
n3 PUFA	19.35 ± 0.09	18.94 ± 0.21	28.27 ± 0.20	27.45 ± 0.12	26.68 ± 0.07	24.28 ± 0.08	40.26 ± 0.08	26.31 ± 0.32	25.25 ± 0.16	29.68 ± 0.02
n6 PUFA	2.47 ± 0.03	2.43 ± 0.03	2.06 ± 0.02	2.09 ± 0.05	2.21 ± 0.01	2.26 ± 0.02	2.62 ± 0.07	1.93 ± 0.04	2.06 ± 0.02	2.08 ± 0.01

The values are mean ± standard deviation of four samples.

^aCatch samples with 80% *Maurolicus muelleri*.

^bCatch samples with 80% *Benthosema glaciale*.

SFAs, saturated fatty acids; MUFAs, monounsaturated fatty acids.

Table 8. Fatty acid composition (% of total fatty acids) in samples (cruise and haul number) collected in 2017 (cruises 2 and 3).

Fatty acid	2-H01 ^a	2-H03	2-H04 ^a	2-H05	3-H01	3-H02 ^a	3-H03	3-H04 ^{a,b}	3-H05	3-H06 ^a	3-H07	3-H08 ^a
Total SFA	31.9 ± 0.28	25.00 ± 0.04	32.20 ± 0.15	27.12 ± 0.14	26.82 ± 0.02	36.56 ± 0.37	21.67 ± 0.09	39.09	37.96 ± 0.63	40.22 ± 0.19	34.20 ± 0.03	39.50 ± 0.22
Total MUFA	21.02 ± 0.06	39.02 ± 0.10	25.06 ± 0.10	39.66 ± 0.38	32.68 ± 0.09	19.53 ± 0.08	36.58 ± 0.24	21.16	20.19 ± 0.52	25.95 ± 0.13	21.19 ± 0.12	22.37 ± 0.08
C20:5n3 EPA	9.77 ± 0.04	8.29 ± 0.04	10.96 ± 0.03	10.39 ± 0.06	10.01 ± 0.01	6.62 ± 0.01	9.79 ± 0.11	6.87	7.69 ± 0.03	6.24 ± 0.04	8.62 ± 0.01	6.65 ± 0.01
C22:5n3 DPA	1.27 ± 0.02	0.42 ± 0.03	1.39 ± 0.01	0.71 ± 0.01	0.67 ± 0.03	0.73 ± 0.01	0.68 ± 0.03	0.61	0.69 ± 0.01	0.70 ± 0.01	0.54 ± 0.01	0.69 ± 0.01
C22:6n3 DHA	30.95 ± 0.38	19.39 ± 0.11	23.99 ± 0.05	13.61 ± 0.09	21.88 ± 0.02	27.07 ± 0.05	24.18 ± 0.45	22.55	25.60 ± 0.24	19.63 ± 0.24	26.98 ± 0.01	22.06 ± 0.04
Total PUFA	47.08 ± 0.39	35.97 ± 0.13	41.73 ± 0.18	33.22 ± 0.12	40.50 ± 0.08	43.90 ± 0.27	41.75 ± 0.47	39.75	41.85 ± 0.31	33.83 ± 0.29	44.61 ± 0.04	38.12 ± 0.09
n3 PUFA	43.93 ± 0.39	31.68 ± 0.12	38.08 ± 0.09	30.06 ± 0.11	36.85 ± 0.04	39.50 ± 0.06	37.98 ± 0.47	35.99	37.77 ± 0.25	30.34 ± 0.25	40.74 ± 0.01	34.73 ± 0.04
n6 PUFA	2.45 ± 0.03	3.41 ± 0.03	2.81 ± 0.09	2.39 ± 0.04	2.59 ± 0.01	3.00 ± 0.05	2.67 ± 0.04	2.66	2.96 ± 0.04	2.42 ± 0.11	(1) 0.04	2.57 ± 0.04

The values are mean ± standard deviation of four samples.

^aCatch samples with 80% *Maurolicus muelleri*.

^bOnly one sample was analysed.

SFAs, saturated fatty acids; MUFAs, monounsaturated fatty acids.

Table 9. Undesirable substances found in five samples collected in 2016 and 2017.

Undesirable substance	Unit	Maximum level in feedstuff, (12% MC)	Maximum level in fish and whole fish (wet weight)	1-H02		1-H07		2-H03		2-H04		3-H05	
				12% MC	Wet weight	12% MC	Wet weight	12% MC	Wet weight	12% MC	Wet weight	12% MC	Wet weight
Arsenic (As)	mg kg ⁻¹	25.0	-	5.87	1.80	7.37	1.90	47.6	7.20	5.59	1.20	7.74	1.90
Cadmium (Cd)	mg kg ⁻¹	2.00	0.05	0.293	0.090	1.71	0.440	1.26	0.190	1.44	0.310	2.85	0.700
Lead (Pb)	mg kg ⁻¹	10.0	0.30	>0.163	>0.05	>0.194	>0.05	>0.331	>0.05	>0.233	>0.05	>0.204	>0.05
Mercury (Hg)	mg kg ⁻¹	0.50	0.50	0.127	0.039	0.116	0.030	0.112	0.017	0.102	0.022	>0.020	>0.005
Sum dioxins and furans	ng kg ^{-1a}	1.25	3.50	0.725	0.222	0.254	0.066	0.457	0.118	0.310	0.080	0.273	0.070
Sum of dioxins and dioxin-like PCBs	ng kg ^{-1a}	4.00	6.50	1.14	0.350	0.413	0.106	0.734	0.189	0.506	0.131	0.439	0.113
Sum non-dioxin-like PCBs	µg kg ⁻¹	30.0	75.0	5.50	1.69	1.76	0.453	2.66	0.686	2.91	0.751	1.59	0.410
Sum endosulfan (alfa-, beta-, sulphate-)	µg kg ⁻¹	100	-	>2.57	>0.787	>3.24	>0.835	>10.4	>1.57	>3.74	>0.803	>3.38	>0.829
Pentachlorobenzene	µg kg ⁻¹	-	-	>0.988	>0.303	>1.24	>0.321	>3.98	>0.602	>1.44	>0.309	>1.30	>0.319
Hexachlorobenzene	µg kg ⁻¹	10.0	-	2.45	0.752	>1.24	>0.321	>3.98	>0.602	>1.44	>0.309	>1.30	>0.319
alfa-HCH	µg kg ⁻¹	20.0	-	>0.492	>0.151	>0.620	>0.160	>1.99	>0.301	>0.722	>0.155	>0.652	>0.160
beta-HCH	µg kg ⁻¹	10.0	-	>0.492	>0.151	>0.620	>0.160	>1.99	>0.301	>0.722	>0.155	>0.652	>0.160
gamma-HCH (lindane)	µg kg ⁻¹	100	-	>0.492	>0.151	>0.620	>0.160	>1.99	>0.301	>0.722	>0.155	>0.652	>0.160
delta-HCH	µg kg ⁻¹	-	-	>0.492	>0.151	>0.620	>0.160	>1.99	>0.301	>0.722	>0.155	>0.652	>0.160
Sum DDT (DDT-, DDD-, DDE-isomers)	µg kg ⁻¹	50.0	-	11.1	3.41	2.58	0.665	5.61	0.848	3.53	0.759	>1.56	>0.383
Aldrin	µg kg ⁻¹	10.0	-	>0.198	>0.061	>0.248	>0.064	>0.794	>0.120	>0.288	>0.062	>0.260	>0.064
Dieldrin	µg kg ⁻¹	10.0	-	4.04	1.24	0.605	0.156	>1.20	>0.181	0.559	0.120	>0.623	>0.153
Endrin	µg kg ⁻¹	10.0	-	>0.593	>0.182	>0.744	>0.192	>2.39	>0.361	>0.866	>0.186	>0.782	>0.192
Sum camphechlor (CHB-26, -52, -62)	µg kg ⁻¹	20.0	-	12.9	3.95	>4.97	>1.28	>15.9	>2.40	>5.75	>1.24	>5.20	>1.28
Heptachlor	µg kg ⁻¹	-	-	>0.198	>0.061	>0.248	>0.064	>0.794	>0.120	>0.288	>0.062	>0.260	>0.064
Mirex	µg kg ⁻¹	-	-	>0.198	>0.061	>0.248	>0.064	>0.794	>0.120	>0.288	>0.062	>0.260	>0.064
Sum chlordane (cis-, trans-, oxy-)	µg kg ⁻¹	20.0	-	3.67	1.13	>1.74	>0.449	>5.57	>0.842	>2.02	>0.435	>1.82	>0.447
Nonachlor, trans-	µg kg ⁻¹	-	-	2.15	0.659	0.388	0.100	>0.398	>0.060	>0.408	>0.088	0.202	0.050
Sum heptachlor epoxide (cis-, trans-)	µg kg ⁻¹	10.0	-	1.00	0.308	>1.12	>0.288	>3.59	>0.542	>1.30	>0.279	>1.17	>0.288
Octachlorostyrene	µg kg ⁻¹	-	-	0.118	0.036	>0.124	>0.032	>0.398	>0.060	>0.144	>0.031	>0.130	>0.032

The results are compared with the EU legislation limits for maximum levels of undesirable substances in feedstuff based on 12% MC and maximum levels in food wet weight. Levels marked with red exceed the maximum levels.

The symbol '>' indicates levels below limit of quantification.

^ang WHO (2005)-TEQ/kg

Mauchline (1982) and Gjosæter (1981) reported high mortality of 2- or 3-year old individuals in summer–autumn that was associated with spawning. *M. muelleri* has an extensive spawning season that runs from April to July in North Atlantic waters (Gjosæter, 1981; Kawaguchi and Mauchline, 1982; Acevedo *et al.*, 2004), although the peak of spawning can vary in relation to latitude (Clarke, 1982; Prosch, 1991). The otolith microstructure analysis indicated that in 2017 the spawning season of *M. muelleri* extended from March to June, with the peak in May. Similarly, Kawaguchi and Mauchline (1982) suggested that *M. muelleri* spawning starts in April–May in the Atlantic Ocean between 48° and 55°N, which is where a large part of our surveys was conducted. In this area, they detected a decrease in the catch of large individuals in summer, which they connected to high mortality after spawning. This scenario could explain our low catch of large individuals in July 2017. Daily growth of *M. muelleri* was estimated by interpreting the otolith increments, but daily deposition had to be assumed due to lack of validation experiments. Little is known about the growth pattern apart from some data reported by Gjosæter (1981), who found high variability in growth and similar ages for individuals ranging from 25 to 47 cm. Armstrong and Prosch (1991) estimated a growth rate of 0.2 mm day⁻¹. Variations in this parameter are common between populations, which supports effects of different environmental conditions. Additionally, the range of fish length can explain high variability in growth.

Gross proximate composition

Our experiments furthermore showed that mesopelagic fish are rich sources of lipids, protein, and minerals with approximate composition of 1.4–15.8 g 100 g⁻¹ lipid, 10.3–16.9 g 100 g⁻¹ protein, and 2.4–3.9 g 100 g⁻¹ ash. Although the proximate gross composition of the raw material varied from haul to haul, some of the constituents were similar to those of other pelagic species such as capelin (*Mallotus villosus*) and atka mackerel (*Pleurogrammus monopterygius*) (Van Pelt *et al.*, 1997), chub mackerel (*Scomber japonicus*) and horse mackerel (*Trachurus trachurus*) (Celik, 2008). Similarly, Sathivel *et al.* (2003) reported that minced whole herring (*C. harengus*) had gross chemical composition of 8.8 g 100 g⁻¹ lipids, 14.5 g 100 g⁻¹ protein, and 3.0 g 100 g⁻¹ ash, and the values for blue whiting (*Micromesistius pou-tassou*) were 2.7–4.2 g 100 g⁻¹ lipids, 16.9–17.5 g 100 g⁻¹ protein, and 3.0–3.1 g 100 g⁻¹ ash (Derkach *et al.*, 2017). Most of our samples contained 15.0 ± 1.5 g 100 g⁻¹ protein, except for haul 2–H03, in which it contributed only 10.3 g 100 g⁻¹ of the raw material. This low protein percentage likely was related to the large percentage of jellyfish in this catch (32.6%). According to Kogovšek *et al.* (2014), jellyfish contain a maximum of 5 g 100 g⁻¹ protein (of dry material), and consequently they may reduce the concentration of protein in mixed hauls. Our results show that the lipid content was significantly influenced by season, as usually is true for fatty fish. The highest lipid content values were obtained in July, and as the lipid content rose, the MC fell (and vice versa). Thus, the sum of moisture and lipids was fairly constant and 82 g 100 g⁻¹ for all hauls, as is also the case for other fatty fish.

Lipid content and omega-3 acids

The large variation in the total lipid class composition is a direct result of the large variation in catch composition between hauls

and cruises. Generally, we observed higher lipid content in larger fish and towards the northern areas. The lipid content obtained from hauls containing 80% fish was generally much higher than that from more mixed hauls with large amounts of krill, jellyfish, cephalopods, and amphipods. In hauls with 80% fish, the amount of lipids and the composition of lipids could be a good source for marine EPA and DHA. High contents of PUFAs EPA and DHA were obtained from those samples, and high levels of phospholipids (PLs) indicated that PLs likely were esterified by n-3 PUFA. In this form, DHA would be bioavailable and absorbed more efficiently and incorporated into different cellular compartments, leading to several positive health effects for consumers (Ramprasath *et al.*, 2015). The lipid composition obtained from hauls with 80% *M. muelleri* had high amounts of FA trophic markers. This finding supports that of Pétursdóttir *et al.* (2008), who suggested that this species preys more heavily on the copepod *Calanus finmarchicus* than *B. glaciale* and therefore that their distributions may be closely correlated. A significant difference between the oil obtained from samples dominated by *M. muelleri* or *B. glaciale* was that the former had high content of triglycerides and the latter contained abundant wax esters. Wax esters include all esters consisting of long chain carboxylic acids with long chain alcohols. Wax esters may be a problem if used in salmon feed, as salmon have limited capacity to utilize them (Olsen *et al.*, 2010). Consequently, oils obtained from *B. glaciale* must be diluted with other oils before being used in aquafeeds. Despite the potential problems with wax esters, PUFAs obtained from mesopelagic fish oils will still be a significant contribution to the unsatisfied demand of marine oils.

Undesirable substances

The level of Cd was above the maximum level for foodstuff in all analysed samples. High levels of Cd were found in samples from hauls with relatively high fractions of *M. muelleri* (1–H07, 97.6%; haul: 2–H04, 94.3%; and haul 3–H05, 63.5%), and therefore such catches would be excluded for direct human consumption. There are some exceptions that allow fish species with higher than the maximum allowed level of Cd to be used as foodstuffs, examples of these are: meat from horse mackerel (*Trachurus* species), mackerel (*Scomber* sp.) and sardine (*Sardina pilchardus*) with levels of 0.10 mg kg⁻¹, anchovy (*Engraulis* sp.) and swordfish (*Xiphias gladius*) with levels of 0.30 mg kg⁻¹ (EC, 2006). Cadmium will primarily be found in the protein fraction, e.g. in the fish meal fraction when producing fish meal and oil, so that oil from *M. muelleri* could nevertheless be used for human consumption. Cadmium in fish feed mainly comes from fishmeal and the content of Cd was below the limits for feedstuff in all samples except for haul 3–H05, suggesting a potential utilization of mesopelagic fish and production of fishmeal for the feed industry. The content of As in haul 2–H3 was above the limits for feedstuff, and Olsen *et al.* (2019) reported a similar results. However, this haul consisted mainly of krill (54.7%) and jellyfish (32.9%); such catch composition has no commercial value due to poor fat or protein content, and consequently it would not be applicable either as food or as feedstuff. A reduction of the catch of these species while targeting mesopelagic fish seems to be the only viable option to reduce these levels of As. The concentration of Pb and Hg in all samples was far below the limits both for food and feedstuff. The concentrations of all other undesirable substances (e.g. various organic pollutants and chlorinated pesticides) were

also far below respective maximum limits both for feedstuff and food.

Considering a Norwegian production of Atlantic salmon (*Salmo salar*) of 1.2 million tonnes in 2016, and the quantity of imported soy protein for use in salmon feed the same year (246,000 tonnes), and based on information from the salmon feed producers, we would need 1.6 million tonnes of mesopelagic fish (with an average protein content of 15%) to fully replace the use of soy protein in salmon feed. A catch of 1.6 million tonnes of mesopelagic fish could also have replaced most of the rapeseed oil in the salmon feed with marine lipids. According to FAOSTAT (2020), the average crop in Brazil, from which Norway imports 80% of the soy, was 2.85 tonnes soybeans hectare⁻¹ in the period 2009–2013. If we assume that the feed conversion ratio for Atlantic salmon is 1.2, there is a need for 1.44 million tonnes of salmon feed for an annually salmon production of 1.2 million tonnes. If we assume that the soy content in the salmon feed is about 23%, the cultivation area for soybeans in Brazil would be equivalent to 116,000 hectares for producing 1.2 million tonnes Atlantic salmon.

While most commercial fish stocks in the North Atlantic are regulated with total allowable catch (TAC) access regulations, individual vessel quotas and bycatch rules, harvesting mesopelagic fish resources, such as *M. muelleri* and *B. glaciale*, will represent a clear exception. As a new mesopelagic fishery may be conducted either as a new- and additional season for today's deep-sea pelagic fleet or by specialized vessels for a year-round mesopelagic fishery, these alternatives represent different capacity adaptations and institutional implications for the management regime in question. Different management principles that could be implemented to a mesopelagic fishery and the interplay to other TAC-regulated pelagic fisheries are discussed in Standal and Grimaldo (2020). Likewise, the profitability of a future mesopelagic fishery would depend on the type and size of the pelagic trawler, the distance to the fishing areas, the price kg⁻¹ of landed mesopelagic fish, the type of strategy (full-time mesopelagic fishery of combined fishery with other commercial pelagic species), seasonality, among other. Since all these variables are unknown, we prefer not to go into such speculative discussion and to keep focus on the quantitative results we have obtained from these cruises.

Conclusion

Results of this study support the existence of a substantial biomass of mesopelagic fish in the NEA. The catch rate of 12 tonnes h⁻¹ consisting mainly of *M. muelleri*, are comparable to catch rates of commercial trawl fisheries on sandeel (*Ammodytes marinus*). The content of valuable marine lipids and protein content found in the unsorted samples, where *M. muelleri* was the main species, is comparable with the nutritional values found in other commercial species such as sandeel, herring (*C. harengus*) and blue whiting (*M. poutassou*), suggesting that *M. muelleri* from the NEA could become a potential source of protein and oil for animal feed and human consumption. If exploited at sustainable levels without impacting biodiversity and compromising the oceans' role in climate regulation, the large biomass of mesopelagic fish could be a valuable source for marine protein with high nutritional value and PUFAs. However, the role of DVM and the biological carbon pump and de facto carbon sequestration must be considered when developing such a fishery. To do this, we need to further assess the role and function of mesopelagic species in

the marine food web and enhance our knowledge about its biomass in space and time.

Supplementary Data

Supplementary material is available at the ICESJMS online version of the manuscript.

Acknowledgements

We are thankful for the excellent cooperation with the crew onboard the pelagic trawler “MS Birkeland” and the financial support of Br. Birkeland Fiskebåtrederi AS, Innovation Norway, the Norwegian Directorate of Fisheries, the Norwegian Seafood Research Fund, and the Research Council of Norway through the industrial research project “Mapping the potential for commercial exploitation of mesopelagic species” for conducting the cruises in 2016 and 2017.

Funding

The EU-project SUMMER (817806) provided financial support for the preparation of this article.

Statement of competing interests

The authors confirm that there is no conflict of interest to declare in this paper.

Data availability statement

The data that support the findings of this study are either published or available from the corresponding author upon reasonable request.

References

- Acevedo, S., Fives, J., and Mohn, C. 2004. Abundance and distribution of the larval stages of the mesopelagic fish *maurolicus muelleri* (Gmelin, 1788) in relation to the hydrography off the west coast of Ireland. ICES Document CM 2004/K: 76.
- Alvheim, A. R., Kjellevold, M., Strand, E., Sanden, M., and Wiech, M. 2020. Mesopelagic species and their potential contribution to food and feed security—a case study from Norway. *Foods*, 9: 344.
- Anderson, C., Brierley, A., and Armstrong, F. 2005. Spatio-temporal variability in the distribution of epi- and meso-pelagic acoustic backscatter in the Irminger Sea, North Atlantic, with implications for predation on *Calanus finmarchicus*. *Marine Biology*, 146: 1177–1188.
- Armstrong, M. J., and Prosch, R. M. 1991. Abundance and distribution of the mesopelagic fish *Maurollicus muelleri* in the southern Benguela system. *South African Journal of Marine Science*, 10: 13–28.
- AOAC. 1990. Official Methods of Analysis of the Association of Official Analytical Chemists. The Association of Analytical Chemists (AOAC), Arlington, VA.
- Benitez-Nelson, C. R., Bidigare, R. R., Dickey, T. D., Landry, M. R., Leonard, C. L., Brown, S. L., Nencioli, F. et al. 2007. Mesoscale eddies drive increased silica export in the subtropical Pacific Ocean. *Science*, 316: 1017–1021.
- Bligh, E. G., and Dyer, W. J. 1959. A rapid method of total lipid extraction and purification. *Canadian Journal of Biochemistry and Physiology*, 37: 911–917.
- Boehlert, G. W., Wilson, D., and Mizuno, K. 1994. Populations of the sternopychid fish *Maurollicus muelleri* on seamounts in the Central North Pacific. *Pacific Science*, 48: 57–69.
- Celik, M. 2008. Seasonal changes in the proximate chemical compositions and fatty acids of chub mackerel (*Scomber japonicus*) and horse mackerel (*Trachurus trachurus*) from the north eastern

- Mediterranean Sea. *International Journal of Food Science and Technology*, 43: 933–938.
- Clarke, T. A. 1982. Distribution, Growth and Reproduction of the Lightfish *Maurolicus muelleri* (Sternoptychidae) off South-East Australia. CSIRO Marine Laboratories. Report 145. Cronulla, NSW, Australia.
- Dalpadado, P., Ellertsen, B., Melle, W., and Skjoldal, H. 1998. Summer distribution patterns and biomass estimates of macrozooplankton and micronekton in the Nordic Seas. *Sarsia*, 83: 103–116.
- Dalpadado, P., and Gjøsaeter, J. 1987. Observations on mesopelagic fish from the Red Sea. *Marine Biology*, 96: 173–183.
- Daukšas, E., Falch, E., Šližytė, R., and Rustad, T. 2005. Composition of fatty acids and lipid classes in bulk products generated during enzymic hydrolysis of cod (*Gadus morhua*) by-products. *Process Biochemistry*, 40: 2659–2670.
- Davison, P., Checkley, D. Jr, Koslow, J., and Barlow, J. 2013. Carbon export mediated by mesopelagic fishes in the northeast Pacific Ocean. *Progress in Oceanography*, 116: 14–30.
- Derkach, S., Grokhovsky, V., Kuranova, L., and Volchenko, V. 2017. Nutrient analysis of underutilized fish species for the production of protein food. *Foods and Raw Materials*, 5: 15–23.
- Dypvik, E., Klevjer, T. A., and Kaartvedt, S. 2012. Inverse vertical migration and feeding in glacier lanternfish (*Bentosema glaciale*). *Marine Biology*, 159: 443–453.
- EC. 2006. <https://eur-lex.europa.eu/eli/reg/2006/1881/2010-07-01>.
- EC. 2002. https://eur-lex.europa.eu/resource.html?uri=cellar:aca28b8c-bf9d-444f-b470-268f71df28fb.0004.02/DOC_1&format=PDF.
- EC. 2011. <https://eur-lex.europa.eu/legal-content/EN/TXT/PDF/?uri=CELEX:32011R1259&from=EN>.
- EC. 2012a. https://ec.europa.eu/jrc/sites/jrcsh/files/Official%20methods%20for%20the%20determination%20of%20heavy%20metals%20in%20feed%20and%20food_v4.pdf.
- EC. 2012b. <https://eur-lex.europa.eu/LexUriServ/LexUriServ.do?uri=OJ:L:2012:091:0001:0007:EN:PDF>.
- EC. 2014. <https://eur-lex.europa.eu/legal-content/EN/TXT/PDF/?uri=CELEX:32014R0488&from=EN>.
- Efron, B. 1982. The Jackknife, the Bootstrap and Other Resampling Plans. SIAM Monograph No. 38, CBMS-NSF. <https://statistics.stanford.edu/sites/g/files/tbjybj6031/f/BIO%2063.pdf>.
- Eigaard, O., Herrmann, B., and Nielsen, J. 2012. Influence of grid orientation and time of day on grid sorting in a small-meshed trawl fishery for Norway pout (*Trisopterus esmarkii*). *Aquatic Living Resources*, 25: 15–26.
- Folkvord, A., Gundersen, G., Albreten, J., Asplin, L., Kaartvedt, S., and Giske, J. 2016. Impact of hatch-date on early life growth and survival of Mueller's pearlside (*Maurolicus muelleri*) larvae, and life history consequences. *Canadian Journal of Fisheries and Aquatic Sciences*, 73: 163–176.
- FAO. 1997. Review of the State of the World Fishery Resources: Marine Fisheries. FAO Fisheries Circular No. 920. Rome. 173 pp.
- FAO. 2014. The State of World Fisheries and Aquaculture 2014: Opportunities and Challenges. Rome. 243 pp.
- FAO. 2016. The State of World Fisheries and Aquaculture: Contributing to Food Security and Nutrition for all. Rome. 200 pp.
- FAOSTAT. 2020. <http://faostat3.fao.org/faostat-gateway/go/to/download/Q/QC/E>.
- Fock, H. O., and Czudaj, S. 2019. Size structure changes of mesopelagic fishes and community biomass size spectra along a transect from the equator to the Bay of Biscay collected in 1966–1979 and 2014–2015. *ICES Journal of Marine Science*, 76: 755–770.
- Fraser, A., Tocher, D., and Sargent, J. 1985. Thin-layer chromatography—flame ionization detection and the quantitation of marine neutral lipids and phospholipids. *Journal of Experimental Marine Biology and Ecology*, 88: 91–99.
- Gamulin, T., and Hure, J. 1985. The distribution of midwater fish *Maurolicus muelleri* (Gmelin) eggs in the jabuka pit region of the Adriatic Sea. *Marine Ecology*, 6: 321–328.
- Geoffroy, M., Daase, M., Cusa, M., Darnis, G., Graeve, M., Santana Hernández, N., Berge, J. *et al.* 2019. Mesopelagic sound scattering layers of the high arctic: seasonal variations in biomass, species assemblage, and trophic relationships. *Frontiers of Marine Science*, 6: 364.
- Gjøsaeter, J. 1981. Life history and ecology of *Maurolicus muelleri* (Gonostomatidae) in Norwegian waters. *Fiskeridirektoratet skrifter (Serie Havundersøkelse)*, 17: 109–131.
- Gjøsaeter, J., Kawaguchi, K. 2002. A Review of the World Resources of Mesopelagic Fish. FAO Fisheries Technical Paper No. 193. 151 pp.
- Gnaiger, E., and Bitterlich, G. 1984. Proximate biochemical composition and caloric content calculated from elemental CHN analysis: a stoichiometric concept. *Oecologia*, 62: 289–298.
- Goodson, M., Giske, J., and Rosland, R. 1995. Growth and ovarian development of *Maurolicus muelleri* during spring. *Marine Biology*, 124: 185–195.
- Godø, O., Patel, R., and Pedersen, G. 2009. Diel migration and swim-bladder resonance of small fish: some implications for analyses of multifrequency echo data. *ICES Journal of Marine Science*, 66: 1143–1148.
- Godø, O. R., Samuelsen, A., Macaulay, G. J., Patel, R., Hjøllø, S. S., Horne, J., Kaartvedt, S. *et al.* 2012. Mesoscale eddies are oases for higher trophic marine life. *PLoS One*, 7: e30161.
- Haberlin, D., Mapstone, G., Mcallen, R., Mcevoy, A. J., and Doyle, T. K. 2016. Diversity and occurrence of siphonophores in Irish coastal waters. *Biology & Environment Proceedings of the Royal Irish Academy*, 116B: 119–129.
- Herrmann, B., Sistiaga, M., Nielsen, K., and Larsen, R. 2012. Understanding the size selectivity of redfish (*Sebastes spp.*) in North Atlantic trawl codends. *Journal of Northwest Atlantic Fishery Science*, 44: 1–13.
- Herrmann, B., Sistiaga, M., Rindahl, L., and Tatone, I. 2017. Estimation of the effect of gear design changes on catch efficiency: methodology and a case study for a Spanish longline fishery targeting Hake (*Merluccius merluccius*). *Fisheries Research*, 185: 153–160.
- Hidalgo, M., and Browman, H. 2019. Developing the knowledge base needed to sustainably manage mesopelagic resources. *ICES Journal of Marine Science*, 76: 609–615.
- Hosia, A., Falkenhaus, T., Baxter, E., and Pages, F. 2017. Abundance, distribution and diversity of gelatinous predators along the northern Mid-Atlantic Ridge: a comparison of different sampling methodologies. *PLoS One*, 12: e0187491.
- Irigoiien, X., Klevjer, T. A., Røstad, A., Martinez, U., Boyra, G., Acuña, J. L., Bode, A. *et al.* 2014. Large mesopelagic fishes biomass and trophic efficiency in the open ocean. *Nature Communications*, 5: 1–10.
- Kaartvedt, S., Staby, A., and Aksnes, D. 2012. Efficient trawl avoidance by mesopelagic fishes causes large underestimation of their biomass. *Marine Ecology Progress Series*, 456: 1–6.
- Kaartvedt, S., Titelman, J., Røstad, A., and Klevjer, T. 2011. Beyond the average: diverse individual migration patterns in a population of mesopelagic jellyfish. *Limnology and Oceanography*, 56: 2189–2199.
- Kaartvedt, S., Torgersen, T., Klevjer, T., Røstad, A., and Devine, J. 2008. Behavior of individual mesopelagic fish in acoustic scattering layers of Norwegian fjords. *Marine Ecology Progress Series*, 360: 201–209.
- Kawaguchi, K., and Mauchline, J. 1982. Biology of myctophid fishes (family Myctophidae) in the Rockall Trough, Northeastern Atlantic Ocean. *Biological Oceanography*, 1: 337–373.
- Kawaguchi, K., and Mauchline, J. 1987. Biology of Sternoptychid fishes Rockall Trough, northeastern Atlantic Ocean. *Biology and Oceanography (NY)*, 4: 99–120.

- Klevjer, T., Irigoien, X., Røstad, A., Fraile-Nuez, E., Benítez-Barrios, V., and Kaartvedt, S. 2016. Large scale patterns in vertical distribution and behaviour of mesopelagic scattering layers. *Scientific Reports*, 6: 19873.
- Kloser, R., Ryan, T., Keith, G., and Gershwin, L. 2016. Deep-scattering layer, gas-bladder density, and size estimates using a two-frequency acoustic and optical probe. *ICES Journal of Marine Science*, 73: 2037–2048.
- Kloser, R., Ryan, T., Young, J., and Lewis, M. 2009. Acoustic observations of micronekton fish on the scale of an ocean basin: potential and challenges. *ICES Journal of Marine Science*, 66: 998–1006.
- Knutsen, T., Hosia, A., Falkenhaus, T., Skern-Mauritzen, R., Wiebe, P., Larsen, R. B., Aglen, A. *et al.* 2018. Coincident mass occurrence of gelatinous zooplankton in Northern Norway. *Frontiers in Marine Science*, 5: 158.
- Kogovšek, T., Tinta, T., Klun, K., and Malej, A. 2014. Jellyfish biochemical composition: importance of standardised sample processing. *Marine Ecology Progress Series*, 510: 275–288. 10.3354/meps10959.
- Li, K. Z., Yin, J. Q., Huang, L. M., and Song, X. Y. 2012. Comparison of siphonophore distributions during the southwest and northeast monsoons on the northwest continental shelf of the South China Sea. *Journal of Plankton Research*, 34: 636–641.
- Lopes, P. C. 1979. Eggs and larvae of *Maurolicus muelleri* (Gonostomatidae) and other fish eggs and larvae from two fjords in western Norway. *Sarsia*, 64: 199–210.
- Melli, V., Herrmann, B., Karlsen, J., Feekings, J., and Krag, L. 2020. Predicting optimal combinations of by-catch reduction devices in trawl gears: a meta-analytical approach. *Fish and Fisheries*, 21: 252–568.
- Mills, C. E. 1995. Medusae, siphonophores, and ctenophores as planktivorous predators in changing global ecosystems. *ICES Journal of Marine Science*, 52: 575–581.
- Naito, Y., Costa, D. P., Adachi, T., Robinson, P. W., Fowler, M., and Takahashi, A. 2013. Unravelling the mysteries of a mesopelagic diet: a large apex predator specializes on small prey. *Functional Ecology*, 27: 710–717.
- Naylor, R., Hardy, R., Bureau, D., Chiu, A., Elliott, M., Farrell, A., Foster, I. *et al.* 2009. Feeding aquaculture in an era of finite resources. *Proceedings of the National Academy of Sciences of the United States of America*, 106: 15103–15110.
- Olsen, R., Strand, E., Melle, W., Nørstebø, J., Lall, S., Ringø, E., Tocher, D. *et al.* 2019. Can mesopelagic mixed layers be used as feed sources for salmon aquaculture? *Deep Sea Research Part II: Topical Studies in Oceanography*.
- Olsen, R., Waagbø, R., Melle, W., Ringø, E., and Lall, S. 2010. Alternative marine resources. *In Fish Oil Replacement and Alternative Lipid Sources in Aquaculture Feeds*, pp. 267–324. Ed. by G. Turchini, W-K. Ng, and D. R. Tocher. CRC Press, Boca Raton, FL.
- Peña, M., Olivar, M., Balbín, R., López-Jurado, J., Iglesias, M., and Miquel, J. 2014. Acoustic detection of mesopelagic fishes in scattering layers of the Balearic Sea (western Mediterranean). *Canadian Journal of Fisheries and Aquatic Sciences*, 71: 1186–1197.
- Pétursdóttir, H., Gislason, A., Falk-Petersen, S., Hop, H., and Svavarsson, J. 2008. Trophic interactions of the pelagic ecosystem over the Reykjanes Ridge as evaluated by fatty acid and stable isotope analyses. *Deep Sea Research Part II: Topical Studies in Oceanography*, 55: 83–93.
- Proud, R., Handegard, N., Kloser, R., Cox, M., and Brierley, A. 2019. From siphonophores to deep scattering layers: uncertainty ranges for the estimation of global mesopelagic fish biomass. *ICES Journal of Marine Science*, 76: 718–733.
- Prosch, R. 1991. Reproductive biology and spawning of the myctophid *Lampanyctodes hectoris* and the sternoptychid *Maurolicus muelleri* in the southern Benguela Ecosystem. *South African Journal of Marine Science*, 10: 241–252.
- Ramprasath, V., Eyal, I., Zchut, S., Shafat, I., and Jones, P. 2015. Supplementation of krill oil with high phospholipid content increases sum of EPA and DHA in erythrocytes compared with low phospholipid krill oil. *Lipids in Health and Disease*, 14: 142.
- Rasmussen, O., and Giske, J. 1994. Life history parameters and vertical distribution of *Maurolicus muelleri* in Masfjorden in summer. *Marine Biology*, 120: 649–664.
- Sathivel, S., Bechtel, P., Babbitt, J., Smiley, S., Crapo, C., Reppond, K., and Prinyawiwatkul, W. 2003. Biochemical and functional properties of herring (*Clupea harengus*) byproduct hydrolysates. *Journal of Food Science*, 68: 2196–2200.
- Scouling, B., Chu, D., Ona, E., and Fernandes, P. 2015. Target strengths of two abundant mesopelagic fish species. *The Journal of the Acoustical Society of America*, 137: 989–1000.
- Sigurdsson, T., Jonsson, G., and Pálsson, J. 2002. Deep scattering layer over Reykjanes Ridge and in the Irminger Sea. *ICES Document CM 2002/M: 09*.
- Šližytė, R., Rustad, T., and Storrø, I. 2005. Enzymatic hydrolysis of cod (*Gadus morhua*) by-products: optimization of yield and properties of lipid and protein fractions. *Process Biochemistry*, 40: 3680–3692.
- Sosulski, F. W., and Imafidon, G. I. 1990. Amino acid composition and nitrogen-to-protein conversion factors for animal and plant foods. *Journal of Agricultural and Food Chemistry*, 38: 1351–1356.
- Staby, A., and Aksnes, D. 2011. Follow the light—diurnal and seasonal variations in vertical distribution of the mesopelagic fish *Maurolicus muelleri*. *Marine Ecology Progress Series*, 422: 265–273.
- Standal, D., and Grimaldo, E. 2020. Institutional nuts bolts for a mesopelagic fishery in Norway. *Marine Policy*, 119: 104043.
- Sutton, T. T., Porteiro, F. M., Heino, M., Byrkjedal, I., Langhelle, G., Anderson, C. I. H., Horne, J. *et al.* 2008. Vertical structure, biomass and topographic association of deep-pelagic fishes in relation to a mid-ocean ridge system. *Deep Sea Research Part II: Topical Studies in Oceanography*, 55: 161–184.
- Valinassab, T., Pierce, G. J., and Johannesson, K. 2007. Lantern fish (*Benthosema pterotum*) resources as a target for commercial exploitation in the Oman Sea. *Journal of Applied Ichthyology*, 23: 573–577.
- Van Pelt, T., Piatt, J., Lance, B., and Roby, D. 1997. Proximate composition and energy density of some north pacific forage fishes. *Comparative Biochemistry and Physiology Part A: Physiology*, 118: 1393–1398.
- Walsh, M., Hopkins, P., Witthames, P., Greer Walker, M., and Watson, J. 1990. Estimation of total potential fecundity and atresia in the western mackerel stock in 1989. *ICES Document CM 1990/H: 31*.
- Young, J., Blaber, S., and Rose, R. 1987. Reproductive biology of three species of midwater fishes associated with the continental slope of eastern Tasmania. *Australia. Marine Biology*, 95: 323–332.
- Zenteno, J. I., Bustos, C. A., and Landaeta, M. F. 2014. Larval growth, condition and fluctuating asymmetry in the otoliths of a mesopelagic fish in an area influenced by a large Patagonian glacier. *Marine Biology Research*, 10: 504–514.

Handling editor: Roland Proud